Heliyon

Glucosamine/L-lactide copolymers as potential carriers for the development of a sustained rifampicin release system using *Mycobacterium smegmatis* as a tuberculosis model

Jorge Ragusa [a,b], **Daniela Gonzalez** [a,b], **Sumin Li** [a], **Sandra Noriega** [a], **Maciej Skotak** [b,1], **Gustavo Larsen** [a,b,*]

[a] *LNK Chemsolutions LLC, 4701 Innovation Drive, Lincoln, NE, 68521, USA*

[b] *Department of Chemical and Biomolecular Engineering, University of Nebraska, Lincoln, NE, 68588-0643, USA*

[*] Corresponding author.

E-mail address: glarsen1@unl.edu (G. Larsen).

[1] Department of Biomedical Engineering, New Jersey Institute of Technology, Newark, NJ, 07102-1982, USA.

Abstract

The present study aims at developing a new, ultrafine particle-based efficient antibiotic delivery system for the treatment of tuberculosis. The carrier material to make the rifampicin (RIF)-loaded particles is a low molecular weight star-shaped polymer produced from glucosamine (core building unit) and L-lactide (GluN-LLA). Particles were made via electrohydrodynamic atomization. Prolonged release (for up to 14 days) of RIF from these particles is reported. Drug release data fits the Korsmeyer-Peppas equation, which suggests the occurrence of a modified diffusion-controlled RIF release mechanism *in vitro* and is also supported by differential scanning calorimetry and drug leaching tests. Cytotoxicity tests on *Mycobacterium smegmatis* showed that antibiotic-free GluN-LLA and polylactides (PLA) particles (reference materials) did not show

any significant anti-bacterial activity. The minimum inhibitory concentration and minimum bactericidal concentration values obtained for RIF-loaded particles showed 2- to 4-fold improvements in the anti-bacterial activity relative to the free drug. Cytotoxicity tests on macrophages indicated that cell death correlates with an increase of particle concentration but is not significantly affected by material type or particle size. Confocal microscopy was used to track internalization and localization of particles in the macrophages. The uptake of GluN-LLA particles is higher than those of their PLA counterparts. In addition, after phagocytosis, the GluN-LLA particles stayed in the cytoplasm and showed favorable long-term drug release behavior, which facilitated the killing of intracellular bacteria when compared to free RIF. The present studies suggest that these drug carrier materials are potentially very attractive candidates for the development of high-payload, sustained-release antibiotic/resorbable polymer particle systems for treating bacterial lung infections.

Keywords: Microbiology, Pharmaceutical chemistry, Pharmaceutical science

1. Introduction

Tuberculosis (TB), a highly contagious disease caused by the *Mycobacterium tuberculosis* (MTB), ranks as the second leading cause of death from an infectious disease worldwide, and has affected 10 million people in 2017 according to the World Health Organization (WHO). In the same year, 1.4 million people died from TB, including 300,000 HIV-positive patients (*Global tuberculosis report 2018. Geneva: World Health Organization*, 2018). *MTB* bacteria that access to a new host via inhaled air can begin the replication process inside the alveolar macrophages (AM) after 2−3 weeks of infection. Macrophages usually ingest and trap pathogens in a phagosome, which is then subject to a series of fusion and fission events within the endocytic pathways that end in phagosome-lysosome fusion. This process in which phagosomes acquire the antimicrobial tools to eliminate the pathogen is known as phagosome maturation. However, *MTB* can modulate pH-reducing events in a maturing phagosome, which can result in a more basic phagolysomal pH, thus facilitating bacteria survival, replication and dormancy of the disease (Gengenbacher and Kaufmann, 2012; Welin and Lerm, 2012). The only treatment currently available for TB, chemotherapy, requires six months of an extensive multi-drug regimen of rifampicin (RIF), isoniazid (INH), pyrazinamide (PYZ), and ethambutol (du Toit et al., 2006). A serious drawback of chemotherapy is the limited bioavailability of the dosed antibiotics in the target area, mainly because its first-pass metabolism decreases the amount of drug that gets into the blood stream. As a consequence, to achieve therapeutic levels, large doses of drugs are normally needed, which in turn increases the probability of side effects (Suarez et al., 2001). Hepatotoxicity,

one the most common side effects of anti-TB drugs, generally leads to treatment withdrawal and discontinuation (du Toit et al., 2006; Tostmann et al., 2008). This long, intensive and commonly toxic treatment is one of the main causes for low patient compliance. Failure to adhere to the prescribed drug regime has resulted in the significant emergence of multi-drug resistant TB (MDR-TB) strains of *MTB*. Treatment of MDR-TB takes longer than conventional TB treatment modalities (WHO recommends 20 months), and requires more expensive and toxic drugs with lower success rates (Cohen et al., 2003; Rakotonirina et al., 2009; Y. Zhang and Yew, 2009). These difficulties are the main driver behind new research aimed at exploring new drug administration concepts.

An alternative strategy to current treatment approaches is to encapsulate anti-TB drugs in nano- or microparticles (MP) made from biodegradable polymers (Hirota et al., 2010; Makino et al., 2004; Mehanna et al., 2014; Ohashi et al., 2009; Vyas et al., 2004). For instance, a very effective particulate treatment should target and undergo endocytosis by AM, and deliver anti-TB drugs where *MTB* is harboring via phagosome maturation arresting (Mehanna et al., 2014; Vyas et al., 2004). Among all the administration routes, inhalation has the inherent benefit of chiefly by-passing first-pass metabolism, thereby allowing elevated local concentrations of the drug where it is most needed, and without requiring high drug concentrations in circulation. This, in turn, reduces systemic toxicity risks (Ranjita et al., 2011). Since alveolar macrophages are one of the first lines of defense against entry of external particles including microbial invasion, AM targeting is generally accomplished even without any specific tailoring of the particles (Fenaroli et al., 2014).

Various drug carriers derived or purified from natural sources such as chitosan (Rajan and Raj, 2012), alginate (Ahmad et al., 2007), gelatin (Manca et al., 2013), and synthetic encapsulants, such as poly(lactide-co-glycolide) (PLGA), poly-D,L-lactide (PDLLA), and polyanhydrides have been used in anti-TB drug encapsulation. RIF is one of the first-line antibiotics being used in TB treatments and is usually employed when investigating new particulate systems. A review of the recent literature on RIF controlled release systems reveals that the most popular proposed drug carriers still belong to PLGA family (Ain et al., 2002; Doan et al., 2011; Doan and Olivier, 2009; Dutt and Khuller, 2001; Hirota et al., 2010; Hong et al., 2008; Ito and Makino, 2004; Makadia and Siegel, 2011; Makino et al., 2004; Pandey et al., 2003; Sharma et al., 2004; Suarez et al., 2001; Tomoda et al., 2005; Yoshida et al., 2006). We have found very few studies reporting on the preparation of MP made from PLA polymers loaded with RIF (Bain et al., 1999; Celikkaya et al., 1996; Coowanitwong et al., 2008; Patomchaiviwat et al., 2008).

The present study aims at developing a RIF loaded-particulate system that delivers the therapeutic in a sustain manner over a long period of time as an alternative treatment of TB. In this work, *in vitro* release of RIF, from submicron particles (SMP)

and MP from a linear LMW and HMW L-lactide, and branched L-lactide grafted glucosamine (GluN-LLA) oligomers produced by electrohydrodynamic atomization (EHDA) was investigated. The custom-made, highly branched biocompatible oligomer, GluN-LLA (Skotak and Larsen, 2010), was processed into SMP and MP, resulting in nearly monodisperse particle size distribution (PSD) systems. For drug delivery applications, three of the most desirable traits of these GluN-LLA oligomers are their high solubility in low toxicity solvents, their tunable hydrophobicity-hydrophilicity balance via control of the length of the lactide substituents, and their LMWs. Cytotoxicity effects of L-lactide, and GluN-LLA base particles on macrophages; and the bactericidal activity of encapsulated and free RIF toward the chosen model microorganism, *Mycobacterium smegmatis* (*M. smegmatis*), were evaluated. *M. smegmatis* is a non-pathogenic and fast-growing species (generation times of 3−4 hours) that shares 2,000 homologs with *MTB*, which makes this microorganism the most accepted model to study *MTB* (Reyrat and Kahn, 2001). The effects produced by the polymeric matrix were evidenced by the minimum inhibitory concentration (MIC) and minimum bactericidal concentration (MBC) values. Confocal microscopy was used to determine the internalization and intracellular location of L-lactide and GluN-LLA based particles containing RIF into macrophages. Finally, the intracellular killing of *M. Smegmatis* in AM showed that the particles are able to maintain a sustained release of RIF into the cells with release rates affecting the bacteria death rate, further pointing to the potential of GluN-LLA as a possible new drug carrier for the treatment of TB.

2. Materials and methods

2.1. Materials

Rifampicin (RIF, >97% HPLC), D-(+)-Glucosamine hydrochloride (GluN-HCl, min. 99%), ethyl acetate (EA, 99.8%) and methanesulfonic acid (MSA, >99.5%) were from Sigma-Aldrich, and ethanol (>99.5%) was received from McCormick Distilling Co., Inc. High molecular weight poly-L-lactide (HMW PLA, NatureWorks Ingeo™ 8302D) with M_n = 123 kDa and polydispersity (PDI) 1.75 (GPC) was purchased from Jamplast, Inc. The L-lactide (LLA, 98%, Alfa) was recrystallized from toluene, vacuum-filtered in an argon atmosphere, vacuum-dried, and stored in a desiccator. All the other chemicals and reagents were purchased from Sigma-Aldrich except where indicated. The low molecular weight poly-L-lactide and GluN-LLA polymer synthesis is described in the following section.

2.2. Polymer synthesis

Low molecular weight poly-L-lactide (LMW PLA, M_n = 2,500 Da, PDI = 1.4 (GPC)) was synthesized according to a procedure published elsewhere (Bourissou

et al., 2005). The GluN-LLA (M_n = 3,100 Da (NMR), PDI = 1.47 (GPC)) with average side-chain length of 11 monomeric L-lactide units, was prepared according to a procedure reported earlier (Skotak and Larsen, 2010; Skotak et al., 2008). Briefly, ten mL of MSA were transferred into a 50 mL flask under argon atmosphere and placed in an oil bath kept at 40 °C. Subsequently, 3.5 mmol of GluN-HCl was added and stirred until homogenization. Then, the L-lactide was added to the reaction mixture, and the flask was flushed with argon for 10 minutes to remove the liberated gaseous HCl. Polymerization of L-lactide occurred for four hours, and the reacting mixture was afterwards quenched with an acid-base neutralization solution, as described elsewhere (Skotak et al., 2008). Vacuum filtration and vacuum drying overnight at the ambient temperature were carried out to isolate and dry the product. Samples were stored in a desiccator until use.

2.3. Particle preparation and characterization

2.3.1. Particle preparation

SMP were prepared from a 5% (w/v) GluN-LLA or LMW PLA, while MP were prepared from a 20% (w/v) GluN-LLA or 1% (w/v) HMW PLA. The preparation of polymeric precursor solutions was done by dissolving the corresponding polymers into EA. These solutions were processed into four different sets of particles using a conventional single-nozzle EHDA setup. The resulting particles were labeled as SMP-GluN-LLA, SMP-LLA and MP-GluN-LLA, MP-LLA, respectively. For the preparation of RIF-loaded particles, three different drug loadings were used: 10, 20 and 50 wt%, which correspond to RIF-to-polymer mass ratios of 1:10, 1:5 and 1:1, respectively; the 1:5 and 1:1 ratios were the most studied in the present contribution. The precursor solution was loaded into a Hamilton series 1000 gastight syringe (model 1001, 1 mL), with a 19 gauge blunt needle attached (to serve as the EHDA nozzle). Subsequently, the syringe was mounted on a digital syringe pump (Cole-Parmer 74900-00, Vernon Hills, IL). Voltage differences in the range of 5−15 kV, (Gamma High Voltage Research ES30P-5W/PRG, Ormond Beach, FL) and a nozzle-to-collector distance of 10 cm were used in the course of a typical experiment. Various flow rates in the range of 0.2−0.5 mL/h were tested to find optimal processing conditions in order to make particles with narrow diameter distributions. The particles were deposited onto an aluminum foil collector tightly wrapped around 15 cm OD circular copper disk. The temperature and relative humidity during the collection of particles were approximately 24 °C and 45%, respectively. The collection time was limited to 10 minutes (optimization phase) or extended up to a few days to collect amounts of particles suitable for further studies.

2.3.2. Size and morphology

Particle size and morphology were assessed via scanning electron microscopy (SEM), using a Hitachi S-3000N microscope with an accelerating voltage of 15 kV and working distance of approximately 13 mm. Coating with metallic gold for 2 minutes before SEM characterization was used to enhance the contrast of non-conducting samples. The electrical current inside the chamber of the Technics Hummer II sputter coater was kept constant (10 mA). Statistical analysis of particle size measurements from SEM images was performed on sets of at least 250 counts within each specimen.

2.3.3. Drug encapsulation efficiency

Approximately 40−50 mg of RIF loaded particles were treated with 5 mL of anhydrous ethanol for 10 minutes (L-lactide polymers are not soluble in this solvent, RIF solubility in ethanol is roughly 10 mg/mL). The suspension was then centrifuged, the supernatant transferred to a 30 mL beaker and subsequently diluted to 15 mL. UV-Vis spectra of RIF in ethanol were recorded in the 250−550 nm range, and concentrations were calculated based on the absorption peak at 306 nm. The drug content entrapped within the particles was analyzed with ^{1}H NMR spectroscopy, using deuterated chloroform ($CDCl_3$, 99.8 atom % D, Sigma-Aldrich) as solvent. Characteristic signals of methyl groups of RIF (1.04, 0.89 and 0.62 ppm) and polymer matrices (1.60 ppm) were compared and used to calculate the drug-to-polymer ratio. Particles that were not treated with ethanol were used as reference.

2.3.4. Particle degradation

Polymer degradation studies were performed using a modified PBS solution: water was replaced with deuterated water to facilitate NMR analysis of the released L-lactic acid. First, the pH of the PBS stock solution was adjusted to 7.4 with 1 M HCl, then water was evaporated and the remaining solid was dried under vacuum. Then, the dry PBS powder was dissolved in deuterated water ($D2O$, 99.8 atom % D, Cambridge Isotope Laboratories) for further use. Solid polymeric particles (50 mg) were dispersed in 5.0 mL of deuterated PBS and the suspension was kept in the dark at 37 °C while shaking it. For NMR analysis, 0.5 mL aliquots were drawn every 24 hours and ^{1}H NMR spectra were recorded on a Bruker Avance 500 NMR spectrometer at 500.13 MHz to track the release of L-lactic acid. Following analysis, samples were poured back into their respective particle suspensions. These studies were done in triplicate for all tested particle types, and for 14 consecutive days.

2.3.5. Thermal properties of RIF loaded particles

Differential Scanning Calorimetry (DSC) runs were performed on Q100 machine (TA Instruments, New Castle, USA), calibrated for temperature and heat flow using indium (melting point 156.6 °C and ΔHm, 28.45 J/g, respectively). Two analytical runs (to confirm repeatability) were performed on each sample at a heating rate of 10 °C/min., by ramping temperature from 0 to 300 °C, and the sample compartment was flushed with dry nitrogen flowing at 25 mL/min. An empty hermetic Al pan was used as a reference.

2.3.6. Drug release studies

Drug release studies were performed under "perfect sink" conditions (Ritger and Peppas, 1987). Briefly, a mass equal to 50 mg of RIF-loaded particles was dispersed in 5 mL of phosphate buffered saline (PBS) (n = 3) (pH = 7.4) supplemented with 0.02% of ascorbic acid as an antioxidant (Makino et al., 2004), the vials were kept in a thermostat/shaker at 37.0 ± 0.1 °C in the dark. Samples of 200 µl were extracted from each vial every hour for the first 8 hours, and then every 24 hours, the total volume was kept constant by replacing the extracted sample volume with 200 µl of fresh PBS. RIF content was measured with a Beckman DU-640 spectrophotometer in the 250−550 nm wavelength range. In the past, the RIF release kinetics has been evaluated at the isosbestic point of the drug, and through its quinone degradation product (330 nm) (Bain et al., 1999; Hong et al., 2008). Absorbance values at 310 nm were used to calculate the concentration of RIF in the absence of drug oxidation, which was prevented by addition of ascorbic acid and a lack of sample exposure to light.

2.4. Data fitting and statistical analysis

Data fitting of temporal RIF release profiles was performed using non-linear curve fitting built-in module of the Origin® 9.0 software. Typically, 60% of the data points were used and fitted to the Korsmeyer-Peppas equation (as required by the model) (Ritger and Peppas, 1987). Statistical evaluation was performed using ANOVA test with p-values below 0.05 and 0.01 considered as significant.

2.5. Evaluation of particle effects on bacteria

2.5.1. Bacterial strain

M. smegmatis ATCC 607 was purchased from Hardy Diagnostics (Santa Maria, CA), and cultured at 37 °C with shaking (150 rpm) in Difco Middlebrook 7H9 (BD Diagnostics, Sparks, MD) medium supplemented with 0.5% (v/v) glycerol, 0.05% Tween 80 to prevent clumping, 10 µg/mL cycloheximide to prevent fungal contamination, 50 µg/mL carbenicillin to prevent other bacterial contamination, and ADS (0.5%

bovine serum albumin, 0.01 M dextrose and 0.015 M NaCl). For each experiment, a fresh overnight culture was prepared with a terminal OD600 reading less than 0.4.

2.5.2. Particle toxicity on M. smegmatis

1 Three million colony forming units (cfu) of freshly prepared mycobacteria were inoculated in 10 mL of 7H9 complete medium for 1 hour at 37 °C before the addition of different amounts of particles (0, 300, 600 and 1,200 μg/mL). The cultures were maintained in the oven at 37 °C with continuous shaking at 150 rpm for 24 hours, and then 10 μL of culture was inoculated onto 7H10 agar plates (7H10 agar supplemented with the same ingredients as 7H9 complete medium without Tween 80) without spreading out and incubated at 37 °C for 3 days to produce visible colonies. Mycobacteria in 7H9 complete medium without particles were considered the particle toxicity control. Pictures of agar plates were taken with a digital camera (24 MP resolution), areas of the colonies formed were quantified by ImageJ software.

2.5.3. Determination of minimum inhibitory concentration (MIC)

The MIC of free RIF and RIF loaded particles for *M. smegmatis* were determined by standard macrobroth dilution techniques recommended by the Clinical and Laboratory Standard Institute (CLSI). Briefly, a series of dilutions of free (0, 1, 2, 4, 8, 16, 32, 64, 128, 256, 512 μg/mL) and RIF encapsulated particles (according to 1:5 RIF-to-polymer mass ratio, 0, 5, 10, 20, 40, 80, 160, 320, 640, 1280, 2560 μg of loaded particles/mL, and 1:1 ratio 0, 2, 4, 8, 16, 32, 64, 128, 256, 512, 1024 μg of loaded particles/mL) in 7H9 medium were prepared. Bacterial suspensions were then added to each tube to make final inocula of 3×10^5 cfu/mL; 10 μL of culture from each tube was taken and then placed onto a 7H10 agar plate without spreading it out. The plates were cultured at 37 °C for 3 days before the colonies were analysed. The lowest concentrations of antibiotic formulations that inhibited the visible bacterial growth after 24 hours were assigned as MIC using McFarland turbidity standard value of 0.5 as reference. Minimum bactericidal concentration (MBC) was defined as the minimal concentration which kills at least 99.9% of bacterial population compared with those in control vials.

2.6. Evaluation of particle loading effects on macrophages

2.6.1. Cell line

Mouse macrophage cell line J774A.1 was purchased from ATCC (Manassas, VA). The cells were grown in Dulbecco's modified eagle's medium (DMEM, Global Cell Solutions, Charlottesville, VA) supplemented with 10% fetal bovine serum (FBS, PAA Lab, Westborough, MA) and antibiotics containing 100 units/mL penicillin,

100 μg/mL streptomycin and 250 ng/mL amphotericin B (Lonza, Walkersville, MD) at 37 °C and 5% CO_2 in a humidified incubator.

2.6.2. Cytotoxicity of particles on macrophage cells

WST-8 assay (Dojindo Molecular Technologies, Inc.) was performed per manufacturer's instructions. In brief, J774A.1 macrophages were seeded in 96-well plates at a density of 1×104 cells/well, and incubated with SMP-GluN-LLA, MP-GluN-LLA, SMP-LLA, and MP-LLA (0 (control), 30, 60, 120 and 240 μg/mL) for 3 days at 37 °C in humidified atmosphere (90% humidity), 5% CO_2. WST-8 reagent solution (10 μL) was added to each well without changing medium, and the plates were incubated for 1 hour prior to OD450 measurement with a BioTek Elx800 microplate reader. Viability of J774A.1 cells was determined from the absorbance of WST-8 in the cell suspension and sample without particle exposure is considered as corresponding to 100% viability.

2.6.3. Particle uptake, and intracellular compartmentalization by confocal microscopy

To determine the internalization of particles into macrophages, 4×10^5 cells were seeded in 35mm glass bottom dishes (MatTek, Ashland, MA) and incubated for 48 hours with 120 μg/mL particles labelled with 1% poly-caprolactone-fluorescein conjugate (PCL-fluorescein, Advanced Polymer Inc, Carlstadt, NJ). For these experiments, 1% w/w PCL-fluorescein/polymer was added to the GluN-LLA or PLA solution before particle fabrication. Subsequently, the cells were stained with 100 nM of MitoTracker® or LysoTracker® (Invitrogen, Carlsbad, CA) in serum-free and phenol red-free DMEM for 10 minutes. CellMask™ plasma membrane staining (Invitrogen) was also performed to confirm the particle internalization. Finally, cells were washed and visualized with a confocal microscope (Olympus FV500-IX 81).

2.6.4. Intracellular killing of M. smegmatis

To examine the effects of RIF loaded particles on killing efficiency of *M. smegmatis* in macrophages, 10^5 cells per well were seeded in 24-well plates and allowed to grow for 24 hours before infection. After washing with antibiotics-free medium twice, 20 multiplicity of infection (MOI: ratio of bacteria/cells) of fresh growing *M. smegmatis* was used to infect the cells for 1 hour and then extracellular bacteria were killed by the addition of gentamicin (20 μg/mL). Free (30 μg/mL), or RIF loaded particles (60 μg/mL, according to 1:1 RIF-to-polymer mass ratio), was then loaded into the cell culture with growing medium without antibiotics. After the incubation period, cells were washed and lysed with water and intracellular survival was estimated by plating serially diluted cultures on 7H10 plates. Pictures of agar plates were taken with a digital camera (24 MP resolution) after 3 days, and

the colonies were counted using ImageJ software. To determine the relative popula-
tion of surviving cells after infection, macrophages were stained with the Live/Dead
viability kit (Invitrogen, 4 μM EthD-1 and 2 μM Calcein AM). After 10 minutes of
incubation with dyes, cells were examined with VWR Vistavision Inverted Epifluor-
escence microscope attached to a LissView Imaging system. Cells were then
counted using ImageJ software.

3. Results and discussion

3.1. Particle fabrication: optimization of processing conditions

Due to the fact that ultimately, fully biocompatible drug delivery systems are
desired, particles were prepared using (the relatively less toxic) ethyl acetate solvent
to dissolve GluN-LLA and PLA polymers. Particle size and morphology was char-
acterized by the processing of SEM images with Gimp 2.8 software. We determined
that the simplest way to achieve particle size control was by varying polymer con-
centration. Preliminary tests using the GluN-LLA oligomer were performed at three
different weight/volume percentages: 5, 10 and 15 (Fig. 1), while keeping flow rate
in all cases at 0.5 mL/h. It is clear that at 5 kV, average particle diameters (PDs) in-
crease (0.79, 0.91 and 2.62 μm) with increasing polymer concentration, and the PSD
were relatively broad in all samples (standard deviation: 0.94, 1.01, 1.88, respec-
tively). Increasing the processing voltage to 10 kV resulted in decreased average
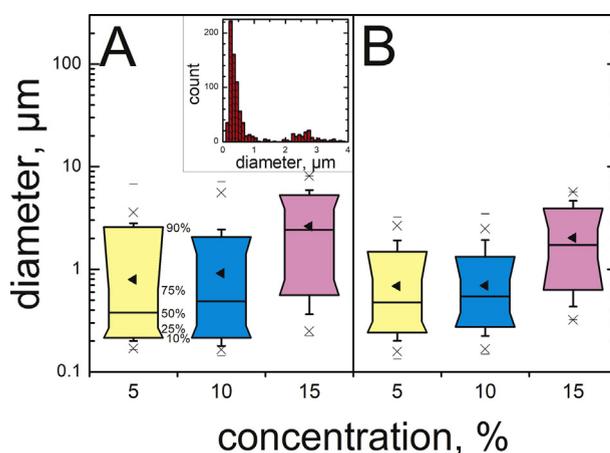PDs (Fig. 1B).

Fig. 1. Control over particle size is achieved by varying the concentration of GluN-LLA. Samples were
solubilized in ethyl acetate and processed at 0.5 mL/h flow rate and voltages of: A) 5 kV, B) 10 kV. With
increasing voltage, the average particle size decreases while particle diameter distribution becomes nar-
rower. Increasing polymer concentration increases the average particle size (◄). Box range: 10−90%,
whisker range: 5−95%, (×) 1−99%, (−) min. and max. values of particle diameter within investigated
population. Inset: bimodal particle size distribution for sample prepared using 5 % w/v GluN-LLA con-
centration. Particle diameter means are significantly different (p < 0.01) at 5kV and 10kV.
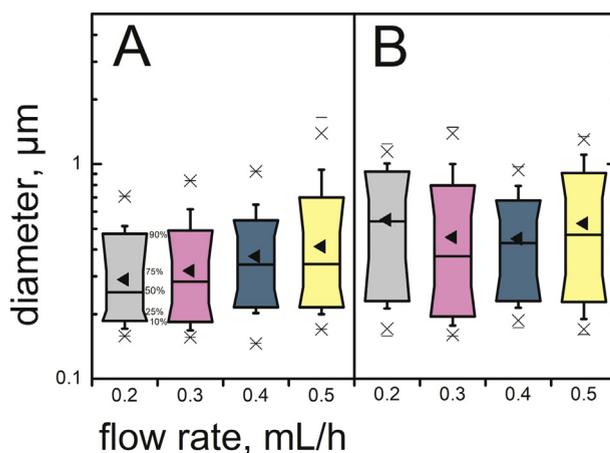
Fig. 2. The effect of processing conditions, flow rate and voltage (A: 5 kV, B: 10 kV) on particle size and distribution. Particles were prepared using a 5% (w/v) solution of GluN-LLA in ethyl acetate. Processing at 5 kV resulted in a bimodal particle size distribution with 80% of the population in sub-micrometer range. Box range: 10–90%, whisker range: 5–95%, (×) 1–99%, (−) min. and max. values of particle diameter within investigated population Box plots present submicron populations exclusively. Particle diameter means are significantly different ($p < 0.01$) at 5kV and 10kV.

The polymer concentration was then fixed at 5 %, and the flow rate was varied from 0.2 to 0.5 mL/h, in 0.1 mL/h increments (Fig. 2). As it turned out, samples processed at 5 kV displayed a bimodal PSD, with 80% of particles being in the submicron region (Fig. 1, inset). This usually is indicative of either the presence of more than one mode of electrified jet breakup, or the occurrence of a "satellite" droplet formation mechanism (Wilhelm et al., 2003). At 10 kV, a practical PSD unimodality was achieved at a flow rate of 0.3 mL/h, with only 3% of population consisting of supra-micron-sized particles. However, a tradeoff between unimodality and PD (if the general goal of using EHDA is indeed making ultrafine particles) becomes apparent, as the former comes at the expense of making larger particles (Fig. 2B). Since in this work our objective was to focus on drug release from well-defined PSDs, we preferred to process our samples at a flow rate of 0.3 mL/h and voltage of 10 kV. Interestingly, increasing the voltage to 15 kV did not lead to smaller PDs. We attribute this effect to a multi-jetting mode being in operation exclusively at 10 kV. The single-jet mode was observed at 5 and 15 kV. The latter leads typically to larger particles relative to cases in which more than one electrified liquid jet is ejected from the Taylor cone. This same trend was also observed during our attempts to optimize the MP design from GluN-LLA and HMW PLA, which suggests that this may be a characteristic of the solvent system, rather than a solute effect.

Table 1. Polymers used in RIF release studies. Type, molecular weight (M_n), processing solution concentration and diameters (average $\pm$ SD) of pure and RIF-loaded particles are presented. Voltage: 10 kV, and flow rate: 0.3 mL/h were used unless specified otherwise.

Polymer	Molecular weight, Da	Concentration, %	Particle diameter, µm			
			Particle type	Pure polymer	1:5[a]	1:1[a]
GluN-LLA	3,100	5.0	SMP-GluN-LLA	0.50 ± 0.30	0.57 ± 0.45	0.90 ± 0.70
		20.0[b]	MP-GluN-LLA	2.10 ± 0.60	—	—
LMW PLA	2,500	5.0	SMP-LLA	0.37 ± 0.30	0.87 ± 0.80	1.22 ± 1.0
HMW PLA	123,000	1.0	MP-LLA	2.90 ± 0.90	—	—

[a] RIF-to-polymer mass ratio used to prepare particles, i.e. 20% and 50% by weight, respectively.
[b] Flow rate 0.5 mL/h was used.

3.2. Fabrication of pure and RIF-loaded submicron- and micron-sized particles

Electrospray, one of the two popular EHDA techniques, was used to develop one-step methods to prepare four sets of particles composed of two different polymeric materials, namely GluN-LLA and PLA. These groups of particles were labeled as SMP-GluN-LLA, MP-GluN-LLA, SMP-LLA, and MP-LLA (Table 1). SMP based on LMW PLA (SMP-LLA) were prepared from their 5% (w/v) solutions in EA at the chosen processing conditions (0.3 mL/h, 10 kV, 10 cm). In order to guarantee complete polymer dissolution and avoid precipitation, the solution needed to remain at
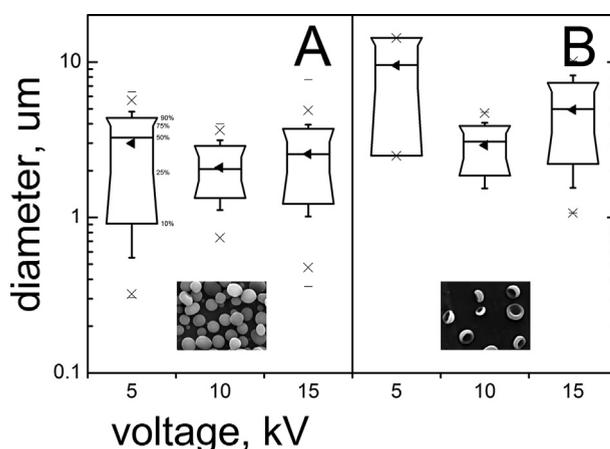

Fig. 3. MP-GluN-LLA (A) and MP-LLA (B) were prepared at discrete voltages as indicated in respective plots. There are statistically significant differences between all populations within the subsets A and B (p < 0.01). Insets show the difference in particle morphology between low and high molecular weight polymers prepared at 10 kV. Spherical MP-GluN-LLA resulted from processing 20% (w/v) GluN-LLA (A). MP-LLA with toroidal shape were obtained by using 1% (w/v) HMW PLA (B). Average particle size (◄), box range: 10−90%, whisker range: 5−95%, (×) 1−99%, (−) min. and max. values of particle diameter within investigated population.

40 °C during processing. For the preparation of SMP-GluN-LLA, a 5% (w/v) GluN-LLA in EA solution was used and processed under the same EHDA conditions. The SMP-LLA presented an average particle diameter slightly smaller than those of their branched counterparts (Table 1). For the preparation of MP-LLA, a concentration of 1% (w/v) of HMWPLA was found to be very close to the polymer's solubility, and that value was selected for sample production under the same processing conditions. MP-GluN-LLA are obtained with 20% (w/v) of GluN-LLA in EA when processed at 0.5 mL/h, 10 kV, and a 10 cm electrode-to-electrode distance.

Fig. 3 shows how voltage affects the PD and PSD of GluN-LLA and PLA MP (Fig. 3A and B, respectively). In this case, a voltage of 10 kV and an emitter-collector distance of 10 cm produce the desired PD and narrow PSD for MP-LLA and MP-GluN-LLA. While MP-GluN-LLA are virtually spherical, MP-LLA shows a toroidal shape which, based on our experience, is indicative of rapid solvent evaporation, that in turn leads to imploded "doughnut"- or "raisin"-shaped particles (Fig. 3, insets). The size and shape of the particles are crucial factors for delivery into the pulmonary airways: particles with aerodynamic diameters between 1-5 μm are preferred (Mohamed & Van Der Walle, 2008; Mortensen et al., 2014). MP with sizes larger than 5 μm are usually deposited in the oral cavity, and SMP particles smaller than <0.5 μm move by Brownian motion and settle slowly. NPs (<100 nm) are not likely to deposit effectively in the pulmonary airways because they are exhaled before deposition (Mortensen et al., 2014). In this work, two size ranges were thus intentionally made: SMP between 0.5 to 0.8 μm and MP between 2 to 3 μm (Table 1). These nearly monodisperse particles were prepared easily, and without using any EHDA apparatus modification. The PD ranges achieved would thus fall within the targeted size ranges for our long-term objective ie., using them for inhalation as mode of drug administration.

To evaluate effects of drug loading on particle morphology and PSD, we performed tests for SMP-GluN-LLA and SMP-LLA at two drug loadings, namely 20 and 50 wt %, which correspond to RIF-to-polymer mass ratios of 1:5 and 1:1, respectively (Figs. 4 and 5). At 20 wt% loading, the broadening of the PSD in this sample (5/1, SMP-LLA) and that of the control differ in a statistically significant manner (*p < 0.01), but this was not observed in the SMP-GluN-LLA sample (Fig. 3A and B). A loading of 50 wt% (5/5) resulted in further PD increases, and in broadening of the PSDs, which could be a consequence of the higher concentration of polymer in the precursor solution. Differences in the PDs of SMP-LLA and SMP-GluN-LLA at a 5/5 polymer to RIF ratio were found to be statistically significant at **p < 0.01. We stress the fact that very high drug loadings and slow release profiles are two extremely desirable traits, and this is exactly the reason why we chose to focus on such high RIF payloads. An increase in general surface irregularities has previously been observed (e.g., particles with wrinkled surfaces) in PLGA MP with increasing RIF loading (Hong et al., 2008). We note however, that this is not indicative of phase
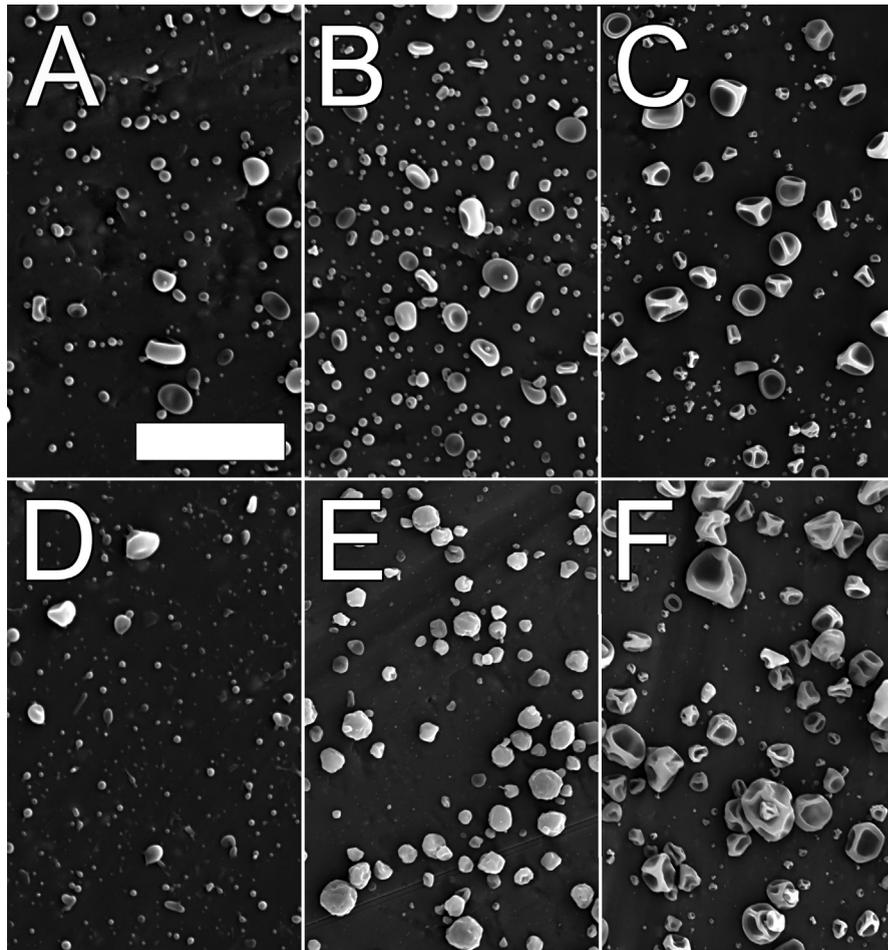
Fig. 4. SEM images illustrating the gradually changing morphology of polymeric submicron particles made of low molecular weight polymers as RIF content is increased: SMP- GluN-LLA (top row) and SMP-LLA (bottom row). Pure polymeric particles (A, D) and with RIF-to-polymer mass ratios of 1:5 (B, E) and 1:1 (C, F) are presented. The scale bar (10 μm) is the same for all images, except E (25 μm).

separation: in our case, separate RIF crystals were never observed by SEM (Fig. 4C, and F).

3.3. Drug encapsulation efficiency

The RIF loading efficiency measured by the EtOH leaching test indicates that the GluN-LLA polymer is superior to its linear homopolymer counterparts irrespective of MW and characteristic dimensions of the particles (Table 2). These results correspond to the amount of RIF retained within the particles at the end of the initial 8-hour period when PBS was used. The entrapment efficiency in the MP is comparable to those of RIF-loaded PLGA MP prepared via the oil-in-water emulsification method (57−78% for PLGAs with MWs 10 and 20 kDa) (Makino et al., 2004). They are also well above those reported with RIF-loaded HMWPLA MP prepared via the supercritical anti-solvent method performed at comparable drug-to-
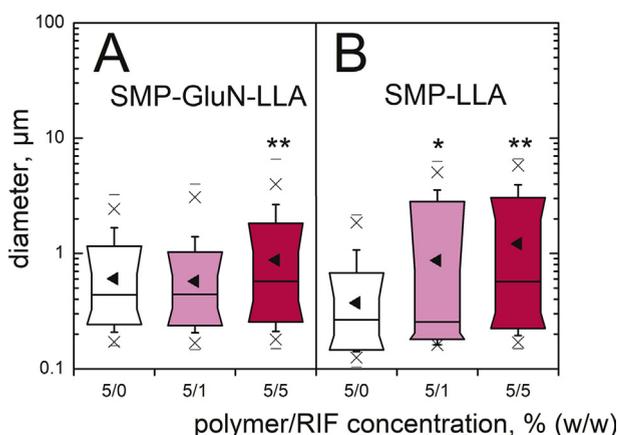
Fig. 5. The effect of RIF loading expressed as polymer-to-RIF mass ratio, average diameter and particle size distribution. Two low molecular weight polymers were tested: A) SMP-GluN-LLA made with branched GluN-LLA, and B) SMP-LLA made with linear LMW PLA. Particles were prepared at a flow rate of 0.3 mL/h and voltage of 10 kV. There are statistically significant differences between SMP-GluN-LLA and SMP-LLA (5/5 polymer to RIF ratio) when compared with their controls, panels A and B (**p < 0.01). At the 5/1 ratio, only the SMP-LLA were statistically significant different when compared with its control (*p < 0.01). Average particle size (◄), box range: 10−90%, whisker range: 5−95%, (×) 1−99%, (−) min. and max. values of particle diameter within investigated population.

Table 2. Encapsulation efficiency and kinetic parameters of RIF release from L-lactide based polymeric submicron and microparticles (n = 3).

Polymer	RIF: polymer ratio	Type	Encapsulation efficiency, %[a]	RIF release efficiency, %[b]	Korsmeyer-Peppas equation fitting results[c]		
					n	*k*	R^2
GluN-LLA	1: 5	SMP-GluN-LLA	56.0 ± 0.1	97.5	0.13	0.29	0.90
	1:10	SMP-GluN-LLA	−	96.6	0.15	0.28	0.90
LMW PLA	1: 5	SMP-LLA	15.0 ± 0.2	98.3	0.71	0.14	0.99
GluN-LLA	1: 5	MP-GluN-LLA	71.0 ± 1.7	93.1	0.14	0.33	0.95
	1: 10	MP-GluN-LLA	−	98.1	0.22	0.25	0.93
HMW PLA	1: 5	MP-LLA	52.0 ± 0.9	99.0	0.10	0.54	0.98

[a] The drug was extracted with pure ethanol for 10 minutes and the remaining solid was analyzed via ^{1}H NMR.

[b] Results based on initial (theoretical) and cumulative drug loading (calculated from *in vitro* release experiments).

[c] $M_t/M_\infty = kt^n$, where *k* is the constant incorporating characteristics of the macromolecular network system and the drug, *n* is the exponent describing release mechanism, M_t/M_∞ is the fraction of the drug released at time *t*.

polymer ratios (40–50%) (Patomchaiviwat et al., 2008). In general, the encapsulation efficiency calculated from cumulative release curves well exceeded 90% for all tested LMW systems (Table 2) but is extremely low for HMWPLA. This is an expected result, as the low degradation rates of this class of polymers often results in permanent drug entrapment inside polymer network (Zeng et al., 2003).

3.4. Particle degradation

The degradation studies performed under identical conditions as those from drug release measurements revealed that L-lactic acid (LLA) release is proportional to the available contact surface between polymeric particles and the solution (Fig. 6). All tested polymers are hydroxyl-terminated and on a molecular level, the degradation mechanism for these polymers is end chain scission (van Nostrum et al., 2004). Both types of SMP exhibited similar degradation curves, but after two weeks the LLA concentration was higher for SMP-GluN-LLA, 8.2×10^{-3} mM, than the 4.0×10^{-3} mM observed with SMP-LLA. Overall, after 14 days, material loss due to degradation of the polymer matrix accounts for only 5% of the initial particulate mass *in vitro*, and thus has negligible effect on the RIF release mechanism.

3.5. Thermal properties: impact on drug release kinetics

1 The DSC measurements revealed that the RIF used in our studies is the stable type I form (a single, sharp exothermic signal, peaking at 253 °C is the only feature in its
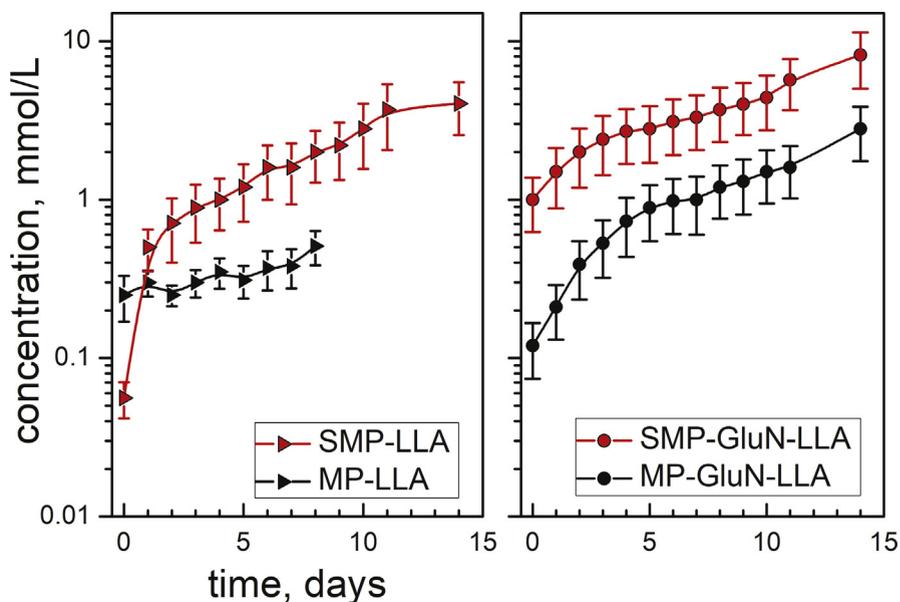

Fig. 6. Semi-log plot of degradation of submicron- (open symbols) and micron-sized particles (filled symbols) prepared using linear (left panel) and branched (right panel) L-lactide based polymers. The release of L-lactic acid was tracked via ^{1}H NMR spectroscopy. Data represent means $\pm$ SE (n = 3).
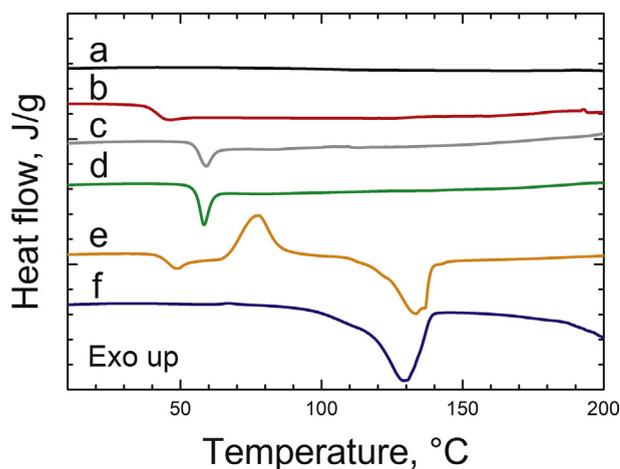
Fig. 7. DSC thermograms. a) RIF, b) as prepared GluN-LLA polymer, c) RIF loaded SMP-GluN-LLA, d) RIF loaded MP-GluN-LLA, e) RIF loaded SMP-LLA f) as prepared LMWPLA. For samples c-e the RIF-to-polymer ratio was 1:5.

thermograms) (S. Agrawal, Ashokraj, Bharatam, Pillai and Panchagnula, 2004). The glass transition temperatures (T_gs) for RIF-loaded SMP and MP prepared with GluN-LLA increased by 8−10 °C when compared to that of the pure polymer (Fig. 7, thermograms b, c and d) (Skotak and Larsen, 2010). This is indicative of enhanced drug-polymer molecular interactions, i.e. RIF likely binds to terminal hydroxyl groups of GluN-LLA chains, thereby increasing its "effective molecular weight", as evidenced by augmented T_g values. On the other hand, introduction of RIF is less likely to be responsible for the observed differences in thermal properties between pure and drug-loaded LMW PLA SMP. The as-prepared material is highly crystalline and there is no obvious characteristic glass transition inflection point seen in its thermogram (Fig. 7f). However, rapid solvent evaporation during processing results in semi-crystalline features: T_g (46 °C) and an exothermic "cold crystallization" peak at 77 °C were followed by an endothermic melting peak at 133 °C. If the drug occupies exclusively the limited available amorphous polymer regions and molecular interactions are thus very weak or absent; then it will be rapidly released upon contact with the PBS solution (Fig. 6) or ethanol (Table 2).

2 Differences in molecular architecture have a pronounced effect on the thermal properties of these polymers: while GluN-LLA is purely amorphous as evidenced by the previously reported DSC results, $T_g = 43.7 \pm 1.3$ °C and the absence of the melting peak of the crystalline phase (Skotak and Larsen, 2010), the LWM PLA possesses semi-crystalline characteristics (Fig. 7f) (Bouapao and Tsuji, 2009). The DSC results suggest that chain length is a decisive crystallinity control factor for oligo-L-lactides, and transition from an amorphous to a semi-crystalline material takes place for monomer numbers higher than 10−12. In view of our results, the advantages of using branched over linear molecular architectures for

RIF delivery applications are apparent. The fine-tuning of the polymeric matrix crystallinity (a strategy that is sometimes used as an important drug release control factor) requires detailed knowledge of its thermal properties, and often demands the use of an additional post-processing step (Jeong et al., 2003). In matrices with reduced crystallinity, such as the purely amorphous GluN-LLA, drug-polymer interactions are enhanced. This, in turn, leads to efficient dispersion of the drug within the polymer matrix, making these systems excellent candidates for applications requiring slow release of the drug (Freiberg and Zhu, 2004). Such systems would indeed be well suited for TB treatment: a typical TB treatment lasts 6 months, and with daily drug doses (du Toit et al., 2006). The *in vitro* drug release performance of our GluN-LLA materials thus warrants future *in vivo* testing and motivated the cell uptake/efficacy studies presented in the paper.

3.6. Rifampicin release from submicron- and microparticles

As mentioned before, the most important concern in conventional TB treatment is patient's low compliance, which is primary based on its duration and intensity, where the affected individual takes a significant number of pills daily for a long time. In this case, a sustained release of RIF for a long period of time would greatly reduce the administration frequency, and eventually increase patient's adherence to the treatment. Fig. 8 shows the cumulative RIF release curves from the four types of particles. For all samples, two stages of RIF release can be identified; an initial one, for up to 8 hours (Fig. 9, Step 1 and Fig. 8, insets), and a delayed phase, lasting from 8 to more than 300 hours (Fig. 9, Step 2 and Fig. 8). The SMP and MP prepared with
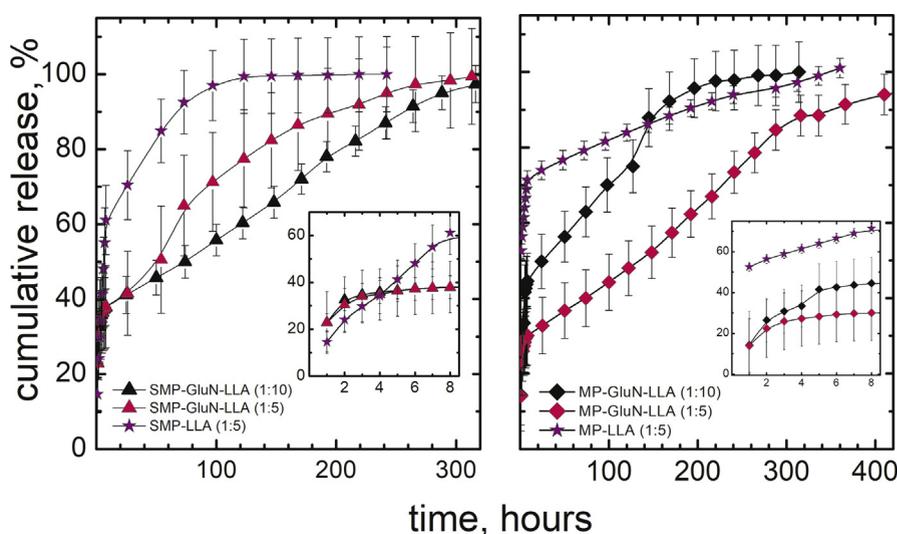

Fig. 8. Cumulative RIF release curves from submicron and microparticles. Release curves correspond to SMP-GluN-LLA (▲), MP-GluN-LLA () with RIF-to-polymer mass ratios of 1:10 and SMP-GluN-LLA (Δ), MP-GluN-LLA (◇), SMP-LLA and MP-LLA (star symbols) with RIF-to-polymer mass ratios of 1:5. Insets show the release profiles during the first 8 hours. Data represent means ± SE (n = 3).
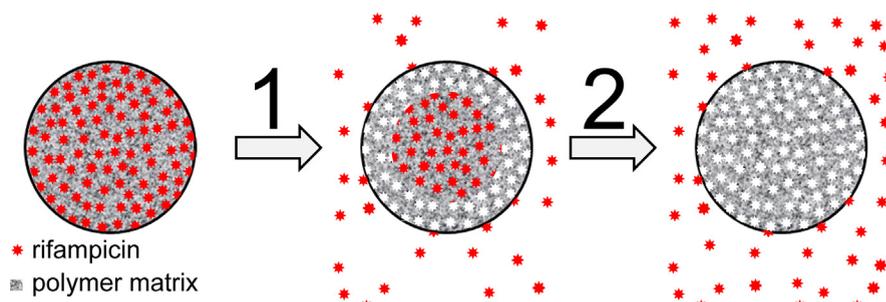
Fig. 9. Representation of the bimodal kinetics of RIF release from the GluN-LLA carrier: 1) initial, 2) delayed. In the delayed phase the drug passes through pores created by molecules released in the initial phase ($k_1 > k_2$). In both phases the effects of drug-polymer interactions were evident and seen as decreased values for the n exponent in the Korsmeyer-Peppas equation (Table 2).

the GluN-LLA material as carrier yielded the desired results i.e., they were able to keep more than 60% of RIF after an initial "burst release", and thus to efficiently release a dominant fraction of the drug over a period of two weeks. We attribute this efficiency to molecular interactions between RIF and the polymeric matrix.

Linear polymers appeared to be less efficient than their branched counterparts in yielding strong molecular interactions with the drug. SMP-LLA prepared using an LMW PLA with a similar molecular weight to that of the GluN-LLA oligomer (Table 1) allowed sustained drug release for 30−40 hours, and as much as 60% of the drug was released within the first 8 hours. MP-LLA, on the other hand, showed 70% RIF release in the first 8 hours, followed by a sustained release over two weeks. Similar results have been reported for PLGA (MW = 5−15 kDa) SMP loaded with budesonide (MW = 430.5 Da) (Y.-H. Lee, Mei, Bai, Zhao and Chen, 2010), and for RIF-loaded PLGA MP (Makino et al., 2004). Increasing particle sizes from 165 nm to 289 nm extended the drug release time from 25-30 hours to 60 hours. Notably, SMP (PDs: 169, 289 and 400 nm) prepared by these authors using a core-shell elec-trospray approach (coaxial, two-liquid nozzle configuration) lost 40−60% of the initial drug payload in just 5 hours. This was found to take place despite the protec-tion provided by a shell made out of PLGA (100% drug encapsulation). We point to the fact that these authors used the same drug release protocols we used in this paper, which is obviously of utmost importance when comparing results from different research groups.

There is little difference between the drug release kinetics from SMP and MP made of GluN-LLA at 10 wt% and 20 wt% payloads (curves SMP-GluN-LLA (1:10) and MP-GluN-LLA (1:5) in Fig. 8, respectively). The ability of our polymers to stabilize high drug payloads is also a most desirable trait, and it suggests the occurrence of a similar release mechanism for both particle diameter groups. This is consistent with particle size-encapsulation efficiency relationships reported by others (Y.-H. Lee et al., 2010).

It is also apparent that the RIF release from SMP-LLA was mechanistically different than that from the GluN-LLA materials. This could be attributed to their different molecular architectures and chemical functionalities, since both polymers have very similar MWs (Table 1). For LMW PLA, the drug release followed an anomalous, non-Fickian diffusion model (n = 0.71, Table 2) as defined by Ritger and Peppas (0.43 < n < 1.00) (Ritger and Peppas, 1987). The Korsmeyer-Peppas equation (see annotation *c* in Table 2 for details) predicts a diffusion-controlled drug release mechanism for systems with diffusion exponent n = 0.43. All tested GluN-LLA submicron- and microparticulate systems have much lower n-values (0.13−0.22, Table 2). This is indicative of drug-polymer matrix interactions, and these results are also consistent with encapsulation efficiency tests and Differential Scanning Calorimetry (DSC) results.

3.7. Particle toxicity on *M. smegmatis*

Chitosan, the polymeric form of glucosamine, has been regarded as having antimicrobial properties (Kong et al., 2010; Tikhonov et al., 2006) with its LMW kind showing the higher bactericidal activity compared to its medium and HMW forms (Melake, Mahmoud, & Al-semary, 2012). Also, the most accepted mechanism of its antibacterial action is believed to involve the positive charge of the protonated amine groups (Liu et al., 2004). For these reasons, we hypothesized a priori that the presence of a glucosamine core (with free amine group, $-NH_2$) in GluN-LLA
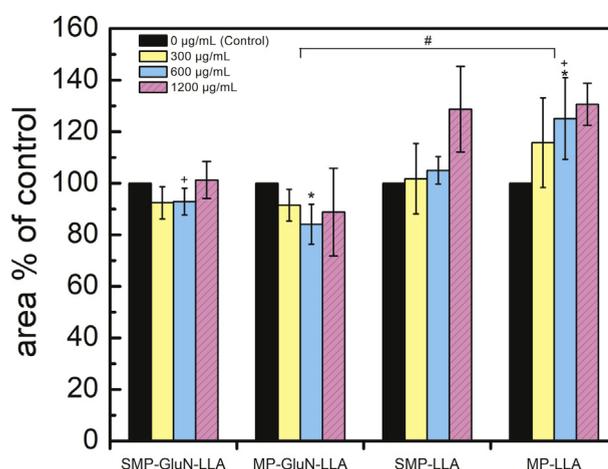

Fig. 10. Toxicity of particles on *M. smegmatis*. Mycobacteria were inoculated with different amounts of submicron- and micron-sized particles and were cultured for 24 hours. 10 μL of culture was placed onto agar plates and incubated at 37 °C for three days to see visible colonies. Colony area was quantified from pictures of agar plates using ImageJ software. Statistically significant differences between SMP-GluN-LLA and MP-LLA ($+p < 0.05$); and between MP-GluN-LLA and MP-LLA ($*p < 0.05$) at a particle concentration of 600 μg/mL, are shown. Statistically significant differences between MP-LLA and MP-GluN-LLA, are indicative of promoted bacterial growth by the linear LLA when compared to the branched GluN-LLA material ($\#p < 0.01$). Data are presented as means ± SE (n = 3).

(Skotak and Larsen, 2010) was possibly going to contribute some antibacterial activity on *M. smegmatis* to the drug-carrier system, but as revealed in Fig. 10, this was not the case. Fig. 10 shows the changes in % growth area compared to control for SMP-GluN-LLA, MP-GluN-LLA, SMP-LLA and MP-LLA at 300, 600 and 1,200 μg of particles/mL. The observed trend was that changes in bactericidal activity for all particle types, and for all concentrations were not statistically different from the control samples. However, there are statistically significant differences among particle materials (MP-GluN-LLA vs MP-LLA, $p < 0.01$): while GluN-LLA particles do not affect bacteria survival; MP-LLA seems to favor *M. smegmatis* growth. This can be explained by the high correlation between microbial adhesion and the hydrophobic/hydrophilic characteristics of the interacting surfaces. In this regard, it has been shown that the adhesion of bacteria to solid surfaces is positively affected by the surface's hydrophobicity (Boks, Norde, van der Mei and Busscher, 2008; Katsikogianni and Missirlis, 2004). Oliveira et al. performed adhesion experiments between different bacteria and polymeric surfaces. These authors found surface hydrophobicity to be proportional to the number of adhering bacteria (Oliveira et al., 2001). Thus, based on the observation that MP-LLA promotes bacterial growth compared to MP-GluN-LLA, we can hypothesize that bacterial adhesion to MP-LLA particles facilitated bacterial proliferation.

3.8. Minimum inhibitory concentration (MIC) and minimum bactericidal concentration (MBC) of free RIF and RIF loaded particles

Table 3 summarizes the MIC and MBC results for free and encapsulated RIF. For particles loaded at a 1:1 RIF-to-polymer mass ratio, SMP-GluN-LLA and MP-GluN-LLA showed MIC values that were about half of that of free RIF on a same dose of antibiotic basis. SMP-LLA showed MIC value 4 times lower than MIC value of RIF alone, while MP-LLA showed MIC value similar to that of RIF alone. MBC values were also affected by encapsulation: SMP-GluN-LLA and SMP-LLA showed

Table 3. MIC and MBC values of RIF in both free and encapsulated form were determined by the macrobroth dilution technique. Particles were produced with a 1:1 RIF-to-polymer mass ratio.

	MIC (1:1) (μg/mL)	MBC (1:1) (μg/mL)
Free RIF	64	256
SMP-GluN-LLA	32	128
MP-GluN-LLA	32	256
SMP-LLA	16	128
MP-LLA	64	256

MBC values 2 times lower than free RIF, while MBC values for MP-LLA and MP-GluN-LLA were unaffected.

Improved efficacy of antibiotics encapsulated in liposomes and intracellular delivery of antibiotics on different microbial strains has been reported. Mirzaee et al. (Mirzaee et al., 2009) have found decreased values of MIC for encapsulated amikacin compared to free amikacin for *E. coli*, *P. aeruginosa*, *S. faecalis* and *S. aureus*. In the same manner, when liposomes were used as encapsulants for amikacin, gentamicin and tobramycin, they reduced the MICs for highly antibiotics-resistant strains, while improving the uptake of antibiotics into the bacterial cells (Halwani et al., 2007). One possible explanation for this phenomenon is membrane fusion between liposomes and bacteria. This would deliver a high dose of antibiotic to the microorganism, and therefore surpass the bacteria efflux pump capacity (Sachetelli et al., 2000; L. Zhang, Pornpattanangku, Hu and Huang, 2010). Another example where the bactericidal effect was also enhanced was shown by the use of RIF-loaded MP. PLGA MP loaded with RIF showed a greater bactericidal effect on *Mycobacterium bovis Bacillus Calmette-Guérin* (BCG) in AM cells than that of RIF in solution when compared at the same periods of time (Hirota et al., 2010). Similar results were obtained by Makino and coworkers (Makino et al., 2004), but in this case higher amounts of RIF were detected inside AM cells treated with RIF-loaded MP than when treated with RIF alone.

MIC reduction in RIF-loaded GluN-LLA and SMP-LLA particles indicates an increase in bacterial killing relative to free RIF. Our tests indicate that antibacterial
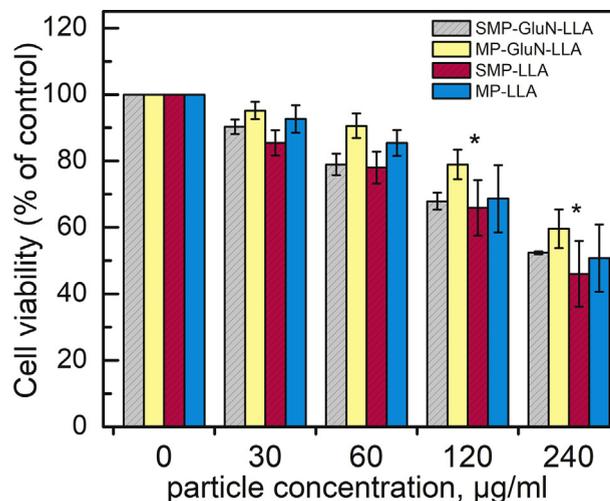

Fig. 11. Particle induced cytotoxicity on macrophages. Different concentrations of GluN-LLA and LLA submicron and microparticles were incubated with macrophages for 3 days. The WST-8 reagent solution was contacted with the samples for one hour prior to OD450 measurement with a BioTek Elx800 microplate reader. Cytotoxicity of submicron and microparticles increased with increasing particle doses. All particle types' cytotoxicity effects were statistically significant in terms of particle concentration when compared to their controls (*$p < 0.05$). Data represent means ± SE (n = 4).

properties of drug-free GluN-LLA and PLA particles on *M. smegmatis* are negligible (Fig. 10). Thus, RIF encapsulation must facilitate endocytosis, resulting in a locally elevated antibiotic concentration.

3.9. Cytotoxicity of particles on macrophage cells

1 In order to determine the cytotoxicity of the four sets of particles, the WST-8 viability assay was implemented. Fig. 11 shows the survival rate (%) of macrophages after three days of incubation with the drug-free (no RIF) particles. Cytotoxicity was shown to be dose dependent i.e., at increasing particle doses there was an increase in cell death. Cytotoxicity was not significantly affected by the material type; at one specific dose level, all particle types showed a very similar effect. When comparing particle concentrations with the control, all particle types showed statistically significant differences at 120 and 240 µg/ml. At a concentration of 60 µg/ml, only SMP-GluN-LLA particles showed significantly different cytotoxicity levels in macrophages relative to the controls. The clear inhibition in macrophages proliferation that occurs at a particle concentration of 120 µg/ml, and at higher values can be due to an accumulation of free lactic acid in the culture media. As a product of polymer degradation, lactic acid could cause a localized, lethal decrease in pH. This has been previously proposed to explain the cytotoxic effect observed with LLA grafted chitosan (Skotak et al., 2008). The cytotoxicity of SMP-GluN-LLA particles at 60 µg/ml (∼20%), could be also correlated with their high cellular uptake (shown in Fig. 12) due to smaller particle size. The increasing number of particles undergoing
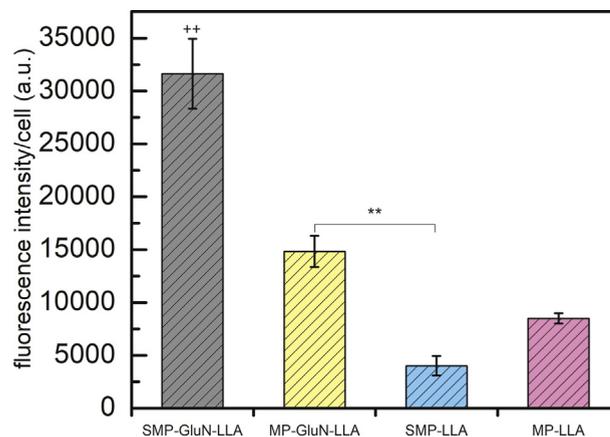

Fig. 12. Internalization of particle by macrophages. Submicron- and micron-sized particles made from GluN-LLA and LLA labeled with PCL-fluorescein were incubated with macrophages. Cells were washed and analyzed with confocal microscopy. The fluorescence intensity/cell of the different types of particles was quantified by ImageJ software. Macrophages showed statistically significant higher SMP and MP uptake made with the branched GluN-LLA polymer than the particles made with the linear LLA polymer. Statistically significant differences (**p < 0.01), and statistically significant differences when comparing with all populations (++p < 0.01) are seen. Data represents means ± SE (n = 4).

endocytosis can lead to an increment in the production of reactive oxygen species (ROS), which is linked to toxicological effects (Nel et al., 2006).

3.10. Particle uptake and intracellular localization

Particle internalization into J774 macrophages was determined by incubation of plasma membrane stained cells with fluorescein-labelled RIF-free particles for 48 hours. Fig. 12 depicts the fluorescence intensity/cell quantified in confocal microscopy images for different types of particles. As noted, macrophages displayed higher internalization of GluN-LLA than PLA particles, with the SMP-GluN-LLA type showing the highest uptake. Particle properties such as hydrophobicity, size, shape, and surface charge affect the cellular uptake (Fröhlich, 2012). Since particle size is similar for the SMP and MP materials (Table 1), the differences between GluN-LLA and PLA could in principle be related to surface properties (charge and hydrophobicity).

To determine the actual location of particles inside cells, confocal microscopy was employed; using optical sectioning technique on macrophages having blue plasma membrane and red lysosome (Fig. 13A), and red mitochondria staining (Fig. 13B), respectively. In these images, stained particles (green) revealed that particles did not colocalize in mitochondria or lysosomes, and after internalization, they remained in the cytoplasm. What we found is of critical relevance to the proposed medical application: the absence of mitochondrial colocalization of particles is extremely desirable. If macrophage targeting is intended, particle colocalization in this organelle is expected to promote oxidative stresses that could lead to cell death. Our results described in the previous sub-section indicate that particle cytotoxicity on macrophages is directly related to particle dose (Fig. 11). However, according to results presented in Fig. 13 particle colocalization cannot be the culprit of these cytotoxic effects. Previous studies showed that PLGA MP loaded with RIF colocalize in phago-lysosomes (Onoshita et al., 2010) suggesting that released RIF molecules diffuse first through the membrane of the phagosomes containing particles to the cytoplasm and then, also by diffusion, enter the phagosomes containing the bacteria. Contrary to this two-step gradient diffusion, a sustained release of RIF directly into the cytoplasm from GluN-LLA particles produces a strong concentration gradient within phago-lysosomes containing bacteria (one step diffusion). Therefore, RIF diffusion through the bacterial membrane and intracellular killing is highly improved. What is also of key relevance to the goals of this study is that GluN-LLA particles showed higher uptakes by macrophages compared to those made of HMW PLA. This property can obviously be very desirable when considering the design of a macrophage-targeting drug delivery system (a K. Agrawal and Gupta, 2000; Terada and Hirota, 2012). Thus, our results demonstrate these polymers meet two important requirements for anti-TB drug delivery applications,

namely: a) high macrophage uptakes and b) dose-dependent, but overall low cytotoxicity.

3.11. Intracellular killing of *M. smegmatis*

2 In order to evaluate the in vitro mycobactericidal effect of RIF-loaded GluN-LLA and PLA particles on *M. smegmatis* inside phagosomes, macrophages were first exposed to a very high MOI of 20 to facilitate infection, and after washing away the extracellular microorganism fraction, infected cells were contacted with RIF loaded particles. Free RIF and no-treatment samples were included in this experiment. The intracellular killing effectiveness of free and encapsulated RIF was determined by the ratio between the number of intracellular bacteria (c.f.u.) and the number of cells alive at the same time point (Fig. 14). The results of no-treatment control experiment are presented as inset in Fig. 14, shows the typical and previously observed cyclical behavior of killing/growth of *M. smegmatis* inside J774A.1 macrophages (Anes et al., 2006; Sonawane et al., 2011). Anes and co-workers observed this cyclic interplay between death and regrowth of *M. smegmatis* bacteria in cultures with MOI values of 5−10, and within 48 hours macrophages managed to successfully eliminate all intracellular bacteria. In order to test the killing efficiency of our sustained release RIF preparations for prolonged period of time (10 days), a very high MOI of 20 was used. Note that in the case of a pathogenic mycobacterium like *MTB*, such high level of infection would naturally cause macrophage apoptosis. Lee and colleagues determined that *MTB* rapidly induces cell apoptosis (90% cells die in merely 20 hours) for MOI > 10. Also, these authors demonstrated that *M. Smegmatis* had a minimal effect on macrophage death at MOI 25 and 50 (J. Lee, Remold, Ieong and Kornfeld, 2006), a characteristic treat that granted long-term infection.

3 We evaluated the antibacterial performance of RIF-loaded particulate systems, and compared it with free RIF for 10 days, using a RIF amount corresponding to half MIC value (Table 3). Free RIF is very effective in killing intracellular bacteria during initial 4 days, as shown by relatively low c.f.u/cell numbers for that period of time (Fig. 14). After day 3, a cyclic pattern is apparent, indicating a reduction in RIF effectiveness. In the case of encapsulated RIF, all systems showed an oscillatory behavior, with a significant reduction in c.f.u/cell values when compared to the control. All tested particulate systems appear to be more efficient in killing bacteria after day 5. This is an expected outcome, and can be explained by the decreased bioavailability of free RIF in culture media at 37 °C, where as much as 50% of the drug is degraded in one week (Yu et al., 2010), while the encapsulated form is protected against these adverse degradation processes. The number of intracellular bacteria per cell in GluN-LLA and PLA polymers seems to be related to the RIF release mechanism (Fig. 8). Both GluN-LLA and SMP-LLA systems presented higher number of intracellular bacteria per cell than free RIF during the first 4 days, but superior
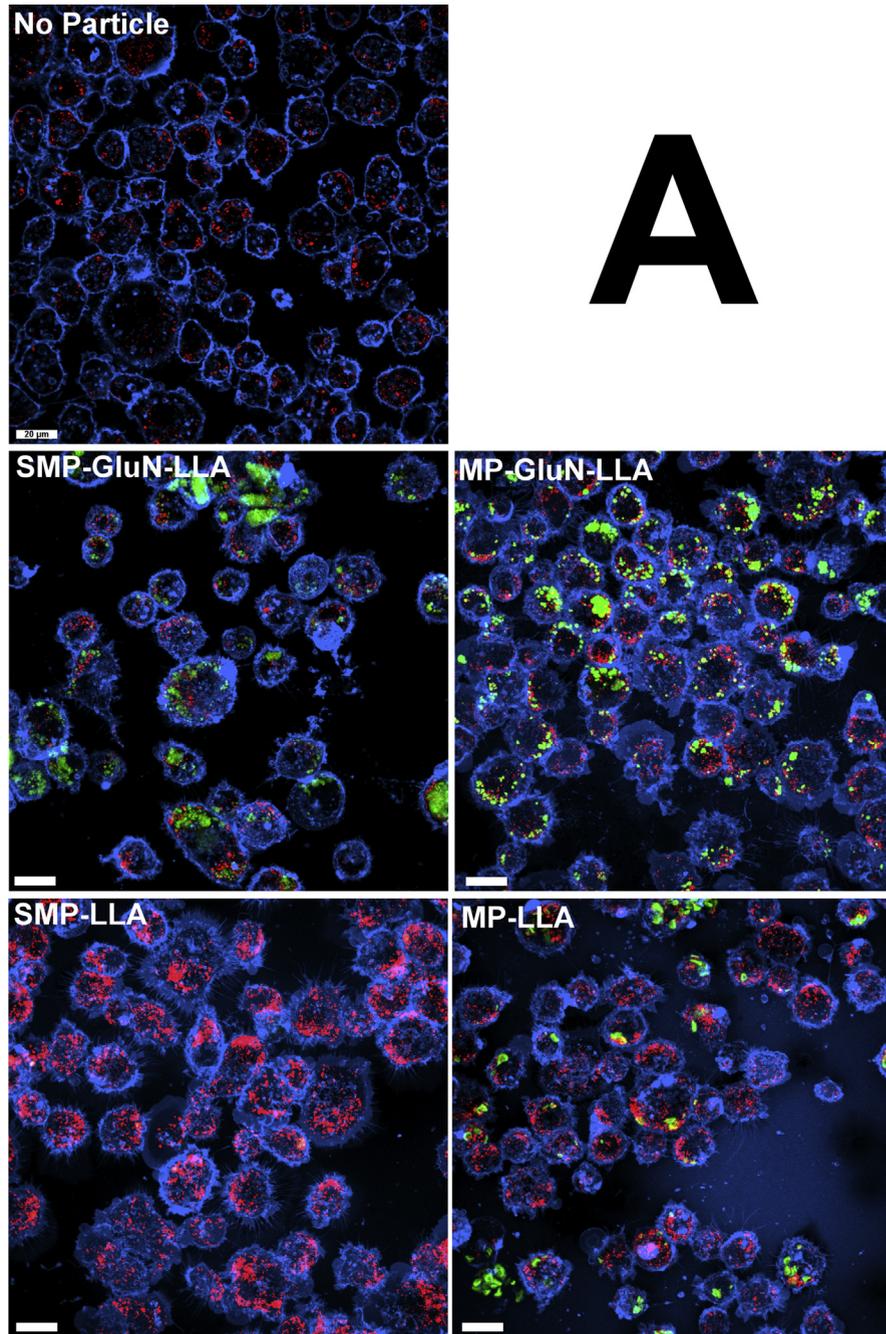
Fig. 13. Intracellular localization of particles. Mitochondria and Lysosome were stained with mitotracker and lysotracker, respectively. In order to be visualized particles containing PCL fluorescein were produced. Part A shows the images of lysosome stained cells: cytoplasm membrane staining (blue) and lysosome staining (red) after incubation with fluorescein loaded particles (green). Part B shows the images of mitochondria stained cells: mitochondria staining (red) after incubation with fluorescein loaded particles (green). Particles are engulfed by the cells, but they do not colocalize either with mitochondria or with lysosomes i.e., they stay in the cytoplasm. The scale bar is 20 μm for all images.
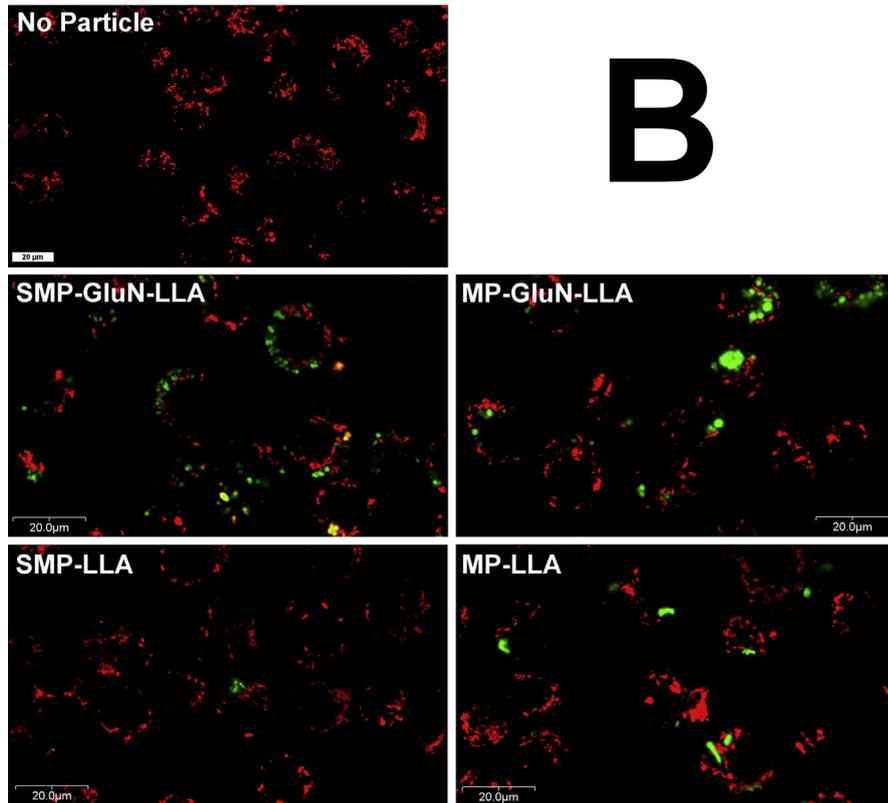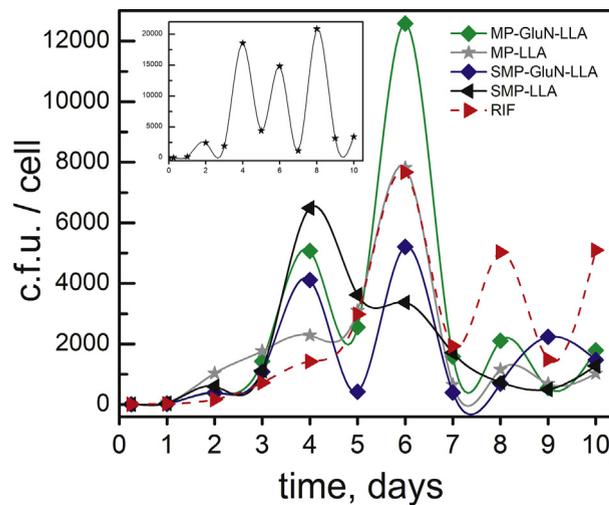
Fig. 13. (*continued*).

Fig. 14. Intracellular killing of *M. smegmatis*. Macrophages were infected with *M. smegmatis* at an MOI of 1:20 (cells:bacteria). After infection macrophages were contacted with free RIF, and or RIF loaded particles. Inset shows control experiments where *M. smegmatis* showed a cyclic growth/killing pattern of colony forming units of intracellular *M. smegmatis* per macrophage cell in terms of time.

killing efficiencies after day 6. On the other hand, the MP-PLA polymer showed a different behavior: similarly, to free RIF, the bioactivity, seen as low c.f.u. per cell numbers, is strongly enhanced during the initial 6 days, which can be attributed to the high burst release of the drug that is characteristic of this system (Fig. 8, $\sim$70% of the drug is released in 8 hours). Our studies demonstrate that careful tailoring of the physicochemical properties of polymeric particles, even these ones, prepared using the same monomer but differing in molecular architecture will allow the design of a delivery system whose drug release profile can be engineered virtually at will.

4 It is worth mentioning that after a thorough literature search, studies assessing effectiveness of RIF-loaded particles in macrophages infected with *M. smegmatis* (as a safe laboratory model to study TB therapeutic strategies) and spanning for more than one day were not found. As one relevant (albeit indirect) example, Sonawane and colleagues (Jena et al., 2012; Mohanty et al., 2013; Sonawane et al., 2011) performed evaluation of antimicrobial properties of several types of starch- and chitosan-coated silver nanoparticles using mouse macrophages infected with *M. smegmatis* (MOI = 10). The study presented in this manuscript seems to have offered, for the first time, results on the long-term (drug release over several days) performance of RIF-loaded ultrafine particles on *M. smegmatis* internalized in macrophages as an arguably more realistic TB model.

4. Conclusion

Using a new biocompatible polymer system based on glucosamine and L-lactide, we have prepared RIF-loaded submicron- and micron-sized particles via an EHDA route. A nearly linear sustained RIF release profile was observed for up to 14 days *in vitro* for GluN-LLA particles. Enhanced RIF-matrix interactions were supported by Korsmeyer-Peppas equation data fitting results, DSC and drug encapsulation efficiency evaluated via ethanol leaching. Four terminal -OH groups and one primary $-NH_2$ group are present in GluN-LLA molecules, as opposed to just a single terminal $-OH$ moiety in the linear PLA. Increased hydroxyl groups density in these polymers is expected to promote matrix-drug interactions via hydrogen bonding. Thus, molecular affinity seemed to have been the dominant release mechanism in our case. Polymers that show high macrophage internalization without co-localization into different organelles are excellent candidates for the production of anti-TB drug carrier particles. This was the case with GluN-LLA based polymers: the drug-loaded particles remain in the cytoplasm, releasing RIF in close proximity to intracellular bacteria. Intracellular killing of *M. smegmatis* by different particles showed a cyclic interplay between live and dead bacteria. The presence of free or encapsulated RIF at sub-MIC concentrations was effective in reducing the number of bacteria per cell compared to the control. It is suggested that the combination

of different particle types and sizes involving at least one type of particle made from the new polymers used in this study will ultimately lead to the design of a system with optimal drug release profiles. Our overarching goal was to design a drug delivery system capable of attacking the microorganism over a long period of time and with just one dose. For a given set of chemical characteristics that could lead to carrier-drug interactions, polymeric materials with higher branching point densities and with amorphous structures may in principle extend RIF release times. The *in vitro* results presented in this paper indicate that GluN-LLA polymeric systems are promising candidates for this particular application.

Declarations

Author contribution statement

Maciej Skotak, Jorge Ragusa: Conceived and designed the experiments; Performed the experiments; Analyzed and interpreted the data; Wrote the paper.

Daniela Gonzalez: Performed the experiments; Analyzed and interpreted the data; Wrote the paper.

Sumin Li: Performed the experiments; Analyzed and interpreted the data.

Sandra Noriega: Conceived and designed the experiments; Performed the experiments; Analyzed and interpreted the data.

Gustavo Larsen: Conceived and designed the experiments; Wrote the paper.

Funding statement

Competing interest statement

The authors declare no conflict of interest.

Additional information

No additional information is available for this paper.

References

Agrawal, a K., Gupta, C.M., 2000. Tuftsin-bearing liposomes in treatment of macrophage-based infections. Adv. Drug Deliv. Rev. 41 (2), 135−146.

Agrawal, S., Ashokraj, Y., Bharatam, P.V., Pillai, O., Panchagnula, R., 2004. Solid-state characterization of rifampicin samples and its biopharmaceutic relevance. Eur. J. Pharm. Sci. 22 (2−3), 127−144.

Ahmad, Z., Sharma, S., Khuller, G.K., 2007. Chemotherapeutic evaluation of alginate nanoparticle-encapsulated azole antifungal and antitubercular drugs against murine tuberculosis. Nanomed. Nanotechnol. Biol. Med. 3 (3), 239−243.

Ain, Q., Sharma, S., Garg, S.K., Khuller, G.K., 2002. Role of poly [DL-lactide-co-glycolide] in development of a sustained oral delivery system for antitubercular drug(s). Int. J. Pharm. 239, 37−46.

Anes, E., Peyron, P., Staali, L., Jordao, L., Gutierrez, M.G., Kress, H., et al., 2006. Dynamic life and death interactions between Mycobacterium smegmatis and J774 macrophages. Cell Microbiol. 8 (6), 939−960.

Bain, D.F., Munday, D.L., Smith, A., 1999. Modulation of rifampicin release from spray-dried microspheres using combinations of poly-(DL-lactide). J. Microencapsul. 16 (3), 369−385.

Boks, N.P., Norde, W., van der Mei, H.C., Busscher, H.J., 2008. Forces involved in bacterial adhesion to hydrophilic and hydrophobic surfaces. Microbiology 154, 3122−3133.

Bouapao, L., Tsuji, H., 2009. Stereocomplex crystallization and spherulite growth of low molecular weight poly(L-lactide) and poly(D-lactide) from the melt. Macromol. Chem. Phys. 210 (12), 993−1002.

Bourissou, D., Martin-Vaca, B., Dumitrescu, A., Graullier, M., Lacombe, F., 2005. Controlled cationic polymerization of lactide. Macromolecules 38 (24), 9993−9998.

Celikkaya, E., Denkbaş, E.B., Pişkin, E., 1996. Rifampicin carrying poly (D,L-lactide)/poly(ethylene glycol) microspheres: loading and release. Artif. Organs 20 (7), 743−751.

Cohen, T., Sommers, B., Murray, M., 2003. The effect of drug resistance on the fitness of Mycobacterium tuberculosis. Lancet Infect. Dis. 3 (1), 13−21.

Coowanitwong, I., Arya, V., Kulvanich, P., Hochhaus, G., 2008. Slow release formulations of inhaled rifampin. AAPS J. 10 (2), 342−348.

Doan, T.V.P., Couet, W., Olivier, J.C., 2011. Formulation and in vitro characterization of inhalable rifampicin-loaded PLGA microspheres for sustained lung delivery. Int. J. Pharm. 414 (1−2), 112−117.

Doan, T.V.P., Olivier, J.C., 2009. Preparation of rifampicin-loaded PLGA microspheres for lung delivery as aerosol by premix membrane homogenization. Int. J. Pharm. 382 (1−2), 61−66.

du Toit, L.C., Pillay, V., Danckwerts, M.P., 2006. Tuberculosis chemotherapy: current drug delivery approaches. Respir. Res. 7 (1), 118.

Dutt, M., Khuller, G.K., 2001. Chemotherapy of Mycobacterium tuberculosis infections in mice with a combination of isoniazid and rifampicin entrapped in Poly (DL-lactide-co-glycolide) microparticles. J. Antimicrob. Chemother. 47 (6), 829−835.

Fenaroli, F., Westmoreland, D., Benjaminsen, J., Kolstad, T., Skjeldal, F.M., Meijer, A., et al., 2014. Nanoparticles as drug delivery system against tuberculosis in zebrafish embryos: direct visualisation and treatment. ACS Nano.

Freiberg, S., Zhu, X.X., 2004. Polymer microspheres for controlled drug release. Int. J. Pharm. 282 (1−2), 1−18.

Fröhlich, E., 2012. The role of surface charge in cellular uptake and cytotoxicity of medical nanoparticles. Int. J. Nanomed. 7, 5577−5591.

Gengenbacher, M., Kaufmann, S.H.E., 2012. Mycobacterium tuberculosis : success through dormancy. FEMS Microbiol. Rev. 36, 514−532.

Global Tuberculosis Report 2018, 2018. World Health Organization, Geneva.

Halwani, M., Mugabe, C., Azghani, A.O., Lafrenie, R.M., Kumar, A., Omri, A., 2007. Bactericidal efficacy of liposomal aminoglycosides against Burkholderia cenocepacia. J. Antimicrob. Chemother. 60 (4), 760−769.

Hirota, K., Hasegawa, T., Nakajima, T., Inagawa, H., Kohchi, C., Soma, G.-I., et al., 2010. Delivery of rifampicin-PLGA microspheres into alveolar macrophages is promising for treatment of tuberculosis. J. Control. Release 142 (3), 339−346.

Hong, Y., Li, Y., Yin, Y., Li, D., Zou, G., 2008. Electrohydrodynamic atomization of quasi-monodisperse drug-loaded spherical/wrinkled microparticles. J. Aerosol Sci. 39 (6), 525−536.

Ito, F., Makino, K., 2004. Preparation and properties of monodispersed rifampicin-loaded poly(lactide-co-glycolide) microspheres. Colloids Surfaces B Biointerfaces 39 (1−2), 17−21.

Jena, P., Mohanty, S., Mallick, R., Jacob, B., Sonawane, A., 2012. Toxicity and antibacterial assessment of chitosan-coated silver nanoparticles on human pathogens and macrophage cells. Int. J. Nanomed. 7, 1805−1818.

Jeong, J.-C., Lee, J., Cho, K., 2003. Effects of crystalline microstructure on drug release behavior of poly(epsilon-caprolactone) microspheres. J. Control. Release 92 (3), 249−258.

Katsikogianni, M., Missirlis, Y.F., 2004. Concise review of mechanisms of bacterial adhesion to biomaterials and of techniques used in estimating bacteria-material interactions. Eur. Cells Mater. 8, 37−57.

Kong, M., Chen, X.G., Xing, K., Park, H.J., 2010. Antimicrobial properties of chitosan and mode of action: a state of the art review. Int. J. Food Microbiol. 144 (1), 51−63.

Lee, J., Remold, H.G., Ieong, M.H., Kornfeld, H., 2006. Macrophage apoptosis in response to high intracellular burden of Mycobacterium tuberculosis is mediated by a novel caspase-independent pathway. J. Immunol. (Baltimore, Md. : 1950) 176, 4267−4274.

Lee, Y.-H., Mei, F., Bai, M.-Y., Zhao, S., Chen, D.-R., 2010. Release profile characteristics of biodegradable-polymer-coated drug particles fabricated by dual-capillary electrospray. J. Control. Release 145 (1), 58−65.

Liu, H., Du, Y., Wang, X., Sun, L., 2004. Chitosan kills bacteria through cell membrane damage. Int. J. Food Microbiol. 95 (2), 147−155.

Makadia, H.K., Siegel, S.J., 2011. Poly lactic-co-glycolic acid (PLGA) as biodegradable controlled drug delivery carrier. Polymers 3 (3), 1377−1397.

Makino, K., Nakajima, T., Shikamura, M., Ito, F., Ando, S., Kochi, C., et al., 2004. Efficient intracellular delivery of rifampicin to alveolar macrophages using rifampicin-loaded PLGA microspheres: effects of molecular weight and composition of PLGA on release of rifampicin. Colloids Surfaces B Biointerfaces 36 (1), 35−42.

Manca, M.L., Cassano, R., Valenti, D., Trombino, S., Ferrarelli, T., Picci, N., et al., 2013. Isoniazid-gelatin conjugate microparticles containing rifampicin for the treatment of tuberculosis. J. Pharm. Pharmacol. 65, 1302−1311.

Mehanna, M.M., Mohyeldin, S.M., Elgindy, N.A., 2014. Respirable nanocarriers as a promising strategy for antitubercular drug delivery. J. Control. Release 187, 183−197.

Melake, N.A., Mahmoud, H.A., Al-semary, M.T., 2012. Bactericidal activity of various antibiotics versus tetracycline-loaded chitosan microspheres against Pseudomonas aeruginosa biofilms. Afr. J. Microbiol. Res. 6 (25), 5387−5398.

Mirzaee, M., Owlia, P., Mehrabi, M., 2009. Comparison of the bactericidal activitiy of amikacin in free and liposomal formulation against Gram-negative and Gram-positive bacteria. Jundishapur J. Nat. Pharm. Prod. 4 (1), 1−7.

Mohamed, F., Van Der Walle, C.F., 2008. Engineering biodegradable polyester particles with specific drug targeting and drug release properties. J. Pharm. Sci. 97 (1), 71−87.

Mohanty, S., Jena, P., Mehta, R., Pati, R., Banerjee, B., Patil, S., Sonawane, A., 2013. Cationic antimicrobial peptides and biogenic silver nanoparticles kill mycobacteria without eliciting DNA damage and cytotoxicity in mouse macrophages. Antimicrobial Agents and Chemotherapy (May).

Mortensen, N.P., Durham, P., Hickey, A.J., 2014. The role of particle physico-chemical properties in pulmonary drug delivery for tuberculosis therapy. J. Micro-encapsul. 31 (8), 785−795.

Nel, A., Xia, T., Mädler, L., Li, N., 2006. Toxic potential of materials at the nano-level. Science (New York, N.Y.) 311 (5761), 622−627.

Ohashi, K., Kabasawa, T., Ozeki, T., Okada, H., 2009. One-step preparation of rifampicin/poly(lactic-co-glycolic acid) nanoparticle-containing mannitol micro-spheres using a four-fluid nozzle spray drier for inhalation therapy of tuberculosis. J. Control. Release 135 (1), 19−24.

Oliveira, R., Azeredo, J., Teixeira, P., Fonseca, A.P., 2001. The Role of Hydropho-bicity in Bacterial Adhesion. BioLine, pp. 11−22, 1952.

Onoshita, T., Shimizu, Y., Yamaya, N., Miyazaki, M., Yokoyama, M., Fujiwara, N., et al., 2010. The behavior of PLGA microspheres containing rifam-picin in alveolar macrophages. Colloids Surfaces B Biointerfaces 76 (1), 151−157.

Pandey, R., Sharma, A., Zahoor, a, Sharma, S., Khuller, G.K., Prasad, B., 2003. Poly (DL-lactide-co-glycolide) nanoparticle-based inhalable sustained drug deliv-ery system for experimental tuberculosis. J. Antimicrob. Chemother. 52 (6), 981−986.

Patomchaiviwat, V., Paeratakul, O., Kulvanich, P., 2008. Formation of inhalable rifampicin-poly(L-lactide) microparticles by supercritical anti-solvent process. AAPS PharmSciTech 9, 1119−1129.

Rajan, M., Raj, V., 2012. Encapsulation, characterisation and in-vitro release of anti-tuberculosis drug using chitosan - poly ethylene glycol nanoparticles. Int. J. Pharm. Pharm. Sci. 4 (4), 255−259.

Rakotonirina, E.C.J., Ravaoarisoa, L., Randriatsarafara, F.M., De Dieu Marie Rakotomanga, J., Robert, A., 2009. Facteurs associés à l'abandon du traitement

anti-tuberculeux dans la ville d'Antananarivo, Madagascar. In: Sante Publique, vol. 21.

Ranjita, S., Loaye, A.S., Khalil, M., 2011. Present status of nanoparticle research for treatment of tuberculosis. J. Pharm. Pharm. Sci. 14 (1), 100−116.

Reyrat, J.-M., Kahn, D., 2001. Mycobacterium smegmatis: an absurd model for tuberculosis? Trends Microbiol. 9 (10), 472−473.

Ritger, P.L., Peppas, N.A., 1987. A simple equation for description of solute release I. Fickian and non-fickian release from non-swellable devices in the form of slabs, spheres, cylinders or discs. J. Control. Release 5 (1), 23−36.

Sachetelli, S., Khalil, H., Chen, T., Beaulac, C., Sénéchal, S., Lagacé, J., 2000. Demonstration of a fusion mechanism between a fluid bactericidal liposomal formulation and bacterial cells. Biochim. Biophys. Acta 1463 (2), 254−266.

Sharma, A., Sharma, S., Khuller, G.K., 2004. Lectin-functionalized poly (lactide-co-glycolide) nanoparticles as oral/aerosolized antitubercular drug carriers for treatment of tuberculosis. J. Antimicrob. Chemother. 54, 761−766.

Skotak, M., Larsen, G., 2010. Visible light-absorbing biocompatible polymers based on L-lactide and aminosugars: preparation and characterization. Polym. Int. 59 (10), 1331−1338.

Skotak, M., Leonov, A.P., Larsen, G., Noriega, S., Subramanian, A., 2008. Biocompatible and biodegradable ultrafine fibrillar scaffold materials for tissue engineering by facile grafting of L-lactide onto chitosan. Biomacromolecules 9 (7), 1902−1908.

Sonawane, A., Santos, J.C., Mishra, B.B., Jena, P., Progida, C., Sorensen, O.E., et al., 2011. Cathelicidin is involved in the intracellular killing of mycobacteria in macrophages. Cell Microbiol. 13, 1601−1617.

Suarez, S., O'Hara, P., Kazantseva, M., Newcomer, C.E., Hopfer, R., McMurray, D.N., Hickey, A.J., 2001. Airways delivery of rifampicin microparticles for the treatment of tuberculosis. J. Antimicrob. Chemother. 48 (3), 431−434.

Terada, H., Hirota, K., 2012. Endocytosis of particle formulations by macrophages and its application to clinical treatment. In: Ceresa, B. (Ed.), Molecular Regulation of Endocytosis.

Tikhonov, V.E., Stepnova, E.A., Babak, V.G., Yamskov, I.A., Palma-Guerrero, J., Jansson, H.-B., et al., 2006. Bactericidal and antifungal activities of a low molecular weight chitosan and its N-/2(3)-(dodec-2-enyl)succinoyl/-derivatives. Carbohydr. Polym. 64 (1), 66−72.

Tomoda, K., Kojima, S., Kajimoto, M., Watanabe, D., Nakajima, T., Makino, K., 2005. Effects of pulmonary surfactant system on rifampicin release from rifampicin-loaded PLGA microspheres. Colloids Surfaces B Biointerfaces 45 (1), 1−6.

Tostmann, A., Boeree, M.J., Aarnoutse, R.E., De Lange, W.C.M., Van Der Ven, A.J.A.M., Dekhuijzen, R., 2008. Antituberculosis drug-induced hepatotoxicity: concise up-to-date review. J. Gastroenterol. Hepatol. 23, 192−202.

van Nostrum, C.F., Veldhuis, T.F.J., Bos, G.W., Hennink, W.E., 2004. Hydrolytic degradation of oligo(lactic acid): a kinetic and mechanistic study. Polymer 45 (20), 6779−6787.

Vyas, S., Kannan, M., Jain, S., Mishra, V., Singh, P., 2004. Design of liposomal aerosols for improved delivery of rifampicin to alveolar macrophages. Int. J. Pharm. 269 (1), 37−49.

Welin, A., Lerm, M., 2012. Inside or outside the phagosome? the controversy of the intracellular localization of *Mycobacterium tuberculosis*. Tuberculosis 92, 113−120.

Wilhelm, O., Madler, L., Pratsinis, S., 2003. Electrospray evaporation and deposition. J. Aerosol Sci. 34 (7), 815−836.

Yoshida, A., Matumoto, M., Hshizume, H., Oba, Y., Tomishige, T., Inagawa, H., et al., 2006. Selective delivery of rifampicin incorporated into poly(DL-lactic-co-glycolic) acid microspheres after phagocytotic uptake by alveolar macrophages, and the killing effect against intracellular Mycobacterium bovis Calmette-Guérin. Microb. Infect. Inst Pasteur 8 (9−10), 2484−2491.

Yu, X., Jiang, G., Li, H., Zhao, Y., Zhang, H., Zhao, L., et al., 2010. Rifampicin stability in 7H9 broth and Lowenstein-Jensen medium. J. Clin. Microbiol.

Zeng, J., Xu, X., Chen, X., Liang, Q., Bian, X., Yang, L., Jing, X., 2003. Biodegradable electrospun fibers for drug delivery. J. Control. Release 92 (3), 227−231.

Zhang, L., Pornpattananangku, D., Hu, C.-M.J., Huang, C.-M., 2010. Development of nanoparticles for antimicrobial drug delivery. Curr. Med. Chem. 17 (6), 585−594.

Zhang, Y., Yew, W.W., 2009. Mechanisms of drug resistance in Mycobacterium tuberculosis. Int. J. Tuberc. Lung Dis. 13 (11), 1320−1330.